

# Micromechanical Optical Modulator

Matt Shepard  
Microelectronic Engineering  
Rochester Institute of Technology  
Rochester, NY 14623

**Abstract**—A novel device was designed and fabricated using Microelectronic and Microelectromechanical systems (MEMS) process procedures. The device was designed to modulate a known wavelength of light using antireflective properties. The mask design was laid out in IC Design portion of Mentor Graphics software package. Device lengths ranging from 150 $\mu$ m to 300 $\mu$ m in length were created including different orientations of etch holes designed for the removal of the sacrificial material. Theoretical modeling of the device, including the applied voltage vs. beam deflection was performed using two-dimensional Fortran program. The result indicates that the smaller devices require a larger amount of voltage than the larger devices, which may be attributed to a larger amount of tension within the beam. A phenomenon called "pull-down" was also observed where the suspended membrane is snapped down to the substrate when the membrane is deflected to 1/3 of the initial gap height. Future work includes the electrical and optical analysis of the devices due to issues associated with the removal of the sacrificial layer.

Index Terms: Optical Modulator, Micromechanical Anti-Reflection Switch (MARS)

## 1. INTRODUCTION

Microelectromechanical Systems or MEMS is the perfect union between conventional mechanical systems, microfabrication, microelectronics and a multitude of creativity. Over the past decade the MEMS industry has evolved into a ~5 billion dollar industry. As of the year 2000, approximately 1% of the industry was concentrated in optoelectronics. In the next few years this number is expected to rise to nearly a third of the total market share. One device, which was developed at Bell Laboratories in 1996, was called the Micromechanical Anti-Reflective Switch (MARS). Its design is geared towards use within the telecommunications industry to increase the speed at which information is relayed into the household. The advantages of using such devices as the MARS device include high speed, temperature insensitivity, and low fabrication cost. The optical modulation device built at

RIT is significantly different in design as compared to Bell Laboratories MARS device. The modified design exploits the high tensile stress of silicon nitride by incorporating a self-suspended silicon nitride dielectric film with a refractive index of ~2.0. The use of this self-suspended membrane greatly simplifies the process of fabrication by eliminating the use of Chemical Mechanical Planarization (CMP) and a Low Pressure Chemical Vapor Deposition (LPCVD) step. The elimination of these two processes effectively drives the cost of production even lower as well as reducing the amount of complexity and variation introduced into the process flow.

The device functions on Fabry-Perot principles, consisting of a reflective silicon substrate and a silicon nitride dielectric film, which are separated by an air gap. For near normal illumination the reflected light is modulated with changes in the gap thickness. The application of a voltage between an aluminum electrode, deposited on top of the silicon nitride film, and the silicon substrate will effectively change the thickness of the air gap. Changes to the air gap thickness will result in a modulation effect on the intensity of the reflected light. In this paper, the investigation of optical modulation, device design simulation, fabrication and analysis of results will be discussed.

## 2. DEVICE DESIGN

The optical modulation device at hand functions by way of a movable anti-reflective membrane suspended over a reflective silicon substrate. Figure 1, shown below is a crosssectional representation of the device.

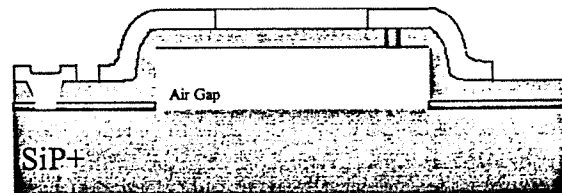


Figure 1: Optical Modulation Device Crosssection

The governing equation for the devices is shown in equation (1), where  $n_0$  ( $n_0=1.0$ ),  $n_g$  ( $n_g=2.0$ ), and  $n_1$

( $n_1=3.5$ ) are the refractive indexes for the air gap, the dielectric film and the substrate respectively. The variable  $h$  denotes the height of the air gap.

$$R = \frac{(n_0^3 - n_1^3 n_g)^2 \sin^2(2\pi h / \lambda) + (n_g n_0^2 - n_1^2 n_0)^2 \cos^2(2\pi h / \lambda)}{(n_0^3 + n_1^3 n_g)^2 \sin^2(2\pi h / \lambda) + (n_g n_0^2 + n_1^2 n_0)^2 \cos^2(2\pi h / \lambda)} \quad (1)$$

The reflectivity,  $R$ , will become a maximum value for  $h=m\lambda/4$  ( $m$ =odd integer). The resulting equation for the maximum reflectivity,  $R_{\max}$ , is shown in (2).

$$R_{\max} = \frac{(n_0^3 - n_1^3 n_g)^2}{(n_0^3 + n_1^3 n_g)^2} \quad (2)$$

Similarly, the minimum reflectance,  $R_{\min}$ , is achieved when the  $h=(m+1)\lambda/4$ . This equation is shown in (3) [5].

$$R_{\min} = \frac{(n_g n_0^2 - n_1^2 n_0)^2}{(n_g n_0^2 + n_1^2 n_0)^2} \quad (3)$$

The chosen dielectric film is silicon nitride with a refractive index of 2.0. Silicon nitride is an excellent candidate for the mechanical structure due to its high tensile stress of a few GPa, which is very close to silicon in strength. The thickness of the film,  $t$ , is denoted by (4), which is dependant upon the material type and the wavelength of incident light,  $\lambda$  [1].

$$t = \frac{m\lambda}{4n} \quad (4)$$

The design of this film is dependant upon the order chosen. For example if  $m=3$  and  $n=2$ , for a HeNe laser source ( $\lambda=632.8\text{nm}$ ), the film thickness required to obtain anti-reflective properties is 237.3nm. This is an optimum choice for this case due to the mechanical requirements of the film. If the film was deposited too thin, it would not hold up in the wet etching performed at the end of the process.

Anti-reflective films function by using interference effects between reflected light waves to effectively deconstruct the wave. The result is the elimination of the reflected light. What is accomplished is a compression of the refracted light wave through the antireflective film (I1), which is then reflected off of the reflective substrate and then decompressed as the light is refracted back into the air. Figure 2 is a representation of this occurrence. The end result is two light waves,  $R_0$  and  $I_2$ , which are exiting the system. A  $\pi$  ( $180^\circ$ ) phase shift is introduced to the two waves, which causes a destructive interference between them. The interference causes the amount of light reflected back from the system to equal zero [4].

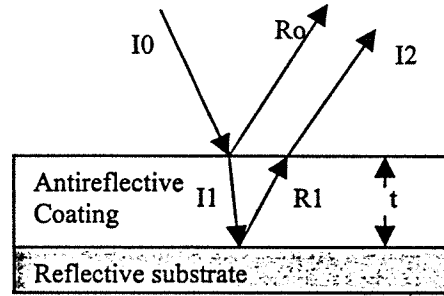


Figure 2: Antireflective Diagram

Now that the antireflective component of the device has been described, the next aspect is how to modulate the reflected light. This is achieved by changing the position of the silicon nitride membrane upon an applied voltage to electrodes, which are partially covering the nitride membrane, and the conductive substrate. The result is the creation of an electrostatic force that will attract the membrane down towards the substrate.

Without any applied voltage, the device has been designed to be in a nominally 'on' state, which theoretically will reflect 75% of the incident light. The thickness of the air gap at this position is 474.6nm. Upon deflection of the beam, a gap height of 316.4nm will reflect ~0% of the incident light turning the device 'off'.

### 3. THEORETICAL SIMULATION

There is an extreme importance of theoretical modeling in MEMS technology. It is very important to develop an idea of the performance of these devices prior to fabrication. To achieve this goal, a two-dimensional simulation program was used to create a plot of the amount of applied voltage vs. beam deflection.

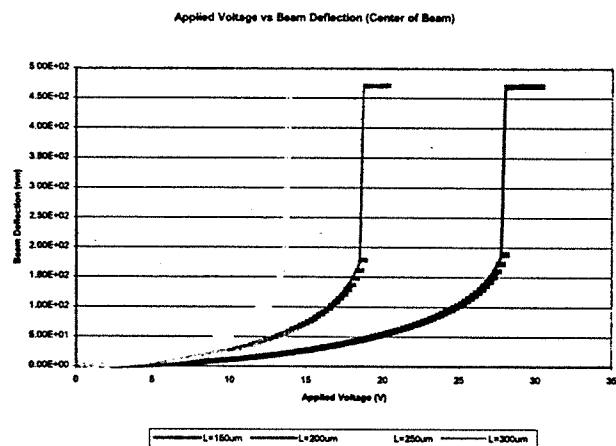


Figure 3: Applied Voltage vs. Beam Deflection

The program used was a Fortran based program developed at Eastman Kodak Co., which allowed the input of several parametric quantities inherent within the modulation devices. A plot of the resulting data extrapolated from the program is shown in Figure 3. The length of the device was varied from 150 $\mu$ m to 300 $\mu$ m. The deflection at the center of the beam was determined vs. the applied voltage for each beam length.

There are two interesting points that are shown in this plot. One is the effect of a phenomenon in MEMS devices called "pull-down." "Pull-down" is described as the theoretical expression that describes what happens to a mechanical structure, such as a beam or cantilever when it gets 1/3 of the initial gap thickness. It obvious from the plot that at ~1/3 of the air gap (158.2nm), each device suffers from the pull-down effect, where the membrane is snapped down to the substrate.

The second point is the effect of the beam size on the voltage required to deflect the beam. The graph shows that the larger beams require less applied voltage for a deflection. This may be attributed to the greater amount of tension in within the smaller beams, which is resisting the applied electrostatic force [1].

#### 4. DEVICE FABRICATION

The process begins with bare P<sup>+</sup> doped wafers. A Low Pressure Chemical Vapor Deposition (LPCVD) of Low Temperature Oxide (LTO) with a thickness of 474.6nm was deposited as the sacrificial layer. Level one lithography was performed using Shipley System 812 photoresist and the GCA g-line stepper using standard coating and developing methods.

The LTO was patterned using a buffered oxide etch (BOE) to make LTO mesas that will form the topography necessary to create the devices. The next process step is to LPCVD the silicon nitride antireflective coating. The thickness of the film is designed to be 237.3nm in thickness to achieve antireflective qualities for a HeNe laser source.

The contact cut lithography, level two, was performed to create a pattern for the Reactive Ion Etch (RIE) silicon nitride etch, which was used to etch a hole for a substrate contact. The chemistry used in the RIE was an SF<sub>6</sub> gas with a power and pressure of 280Watts and 290mtorr respectively. The etch rates observed are near 85.0nm/min. The resist is then stripped in the Bransen asher in an O<sub>2</sub> plasma.

Level three lithography is then performed on the resist for the Aluminum lift-off process. Due to the high acidity of aluminum etchant, it was ruled out as a method of patterning the aluminum lines. Therefore a lift-off process was used as an alternative to aluminum etching. It is important not the hard-bake the resist prior to the evaporation of Aluminum to insure that the resist will be easily removed.

The CHA Evaporator was used to evaporate aluminum on the wafers. Evaporation is the deposition method of choice due to its high level of directional deposition. It is important not to obtain sidewall coverage of the resist to insure that it can be removed in an acetone bath. Had a sputtering mechanism of deposition been used, the aluminum would have been too conformal and the sidewalls of the resist would be covered in aluminum making it impossible to remove the underlying resist.

The resist/aluminum film stack was then removed in an acetone bath. The wafer was soaked in the bath for ~10min. This allowed the resist to break up under the aluminum. The wafer was then sprayed down using a DI water hose. The result was a removal of most of the undesired aluminum. This procedure was performed two to three times to successfully pattern the wafers. Other methods of agitation were explored using an ultrasonic cleaner. The agitation proved to be too aggressive resulting in a good number of the aluminum lines to fall off in a matter of seconds.

After the lift-off patterning process, the wafers were then sintered in the Bruce Furnace at 450°C. This will cause the aluminum to consume the aluminum oxide and create ohmic contacts with high conductivity.

The final lithography level was designed to pattern etch holes in the nitride film. These etch holes are designed to contact the underlying LTO for removal using wet etch chemistries. The same RIE recipe and was performed as the contact cut etch (all RIE processing was performed on the Drytek Quad).

The final process procedure, which proved to be the most difficult, is the removal of the LTO sacrificial layer. The results discussion presents the problems observed with some possible remedies.

#### 5. RESULTS

All processing was completed successfully up until the sacrificial removal step. Due to the inability to achieve a finished product, the results section will discuss the results obtained from the sacrificial etch process.

Several different chemistries were attempted with no conclusion as the optimum method. The first attempt utilized a BOE etchant. BOE was chosen due to its ability to etch LTO without etching silicon nitride. The etch rate on LTO is ~300nm/min while the etch rate on silicon nitride is ~1nm/min. These are purely vertical etch rates on a blanket film. Lateral etch rates achieved for the LTO were 161.3nm/min. After a 30 min etch, it was apparent that the aluminum was beginning to etch in the BOE mixture. Since the devices would need a 4-5 hour etch, it was clear that the aluminum lines would be completely removed.

To eliminate this effect, a mixture of BOE:Ethylene Glycol (5:4) was found to significantly reduce the effects on the aluminum. The resulting lateral etch rate was

reduced to 83.9nm/min as well, which is not acceptable for this process. The lateral distance that the etch needs to clear is 40um which would take over 400min.

As a result of the slow lateral etch rate, a more aggressive approach was taken. Using a mixture of HCL:HF, very high lateral etch rates were achieved at 890nm/min. It is clear that there are some advantages to using this approach, mainly the speed at which the silicon nitride membrane is released. There are two downfalls however. First off the aluminum was etched considerably after 10min and secondly, the etch rate of nitride is near 6nm/min. To alleviate the second problem, the thickness of the nitride needs to be increased to incorporate for the larger etch rates. One other method to overcome the second problem is the additions of several more etch holes throughout the device. The current design does not incorporate nearly enough etch holes to successfully release the silicon nitride membrane. This would decrease the amount of time necessary to remove all of the underlying LTO.

The aluminum line issue is not as easily remedied such as the first iteration with BOE solution. Several mixtures of the HCL:HF etchant mixed with Ethylene Glycol were used to try to decrease the aluminum etch rate. The result was a complete removal of the aluminum lines after 10min of etching. A conclusion was made that an unknown chemical reaction must be occurring to effectively reduce the resilience of aluminum in the HCL:HF solution.

Future work is necessary to develop a solution to the aluminum problem. It may be necessary to reevaluate the chosen materials and decide whether or not a material change is in order. The mask design must also be changed to incorporate a larger number of etch holes.

## 6. CONCLUSION

Optical modulation was not achieved upon the first iteration of the process. Problems were observed at the final step of the procedure. The LTO etch proved to be very difficult with the given materials. The etch rate of the LTO may be increased to an acceptable level however, the metal lines, in this case aluminum, were severely affected by the etch solution. It may be possible to choose a metal that is more resistant to HCL and HF chemistries. Future work will include the experimentation of other possible metals such as Chromium, Titanium, and Tantalum. These three metals are listed as corrosion resistant metals and may incorporate themselves within the given process flow quite well.

## REFERENCES

[1]Furlani, E.P., Lee, E.H., Luo H. "Analysis of Grating Light Valves With Partial Surface Electrodes." *Journal for*

*Applied Physics*. Vol. 83. American Institute of Physics, 1998. Pg. 629.

[2]Goossen, K.W., Walker, J.A. "Fabrication and Performance of MARS Optical Modulators for Fiber-to-the-Home Systems." *SPIE*. Vol. 2879. Page 300.

[3]Goossen, K.W., Walker, J.A., Arney, S. "Fabrication of a Mechanical Antireflection Switch for Fiber-to-the Home Systems." *Journal of Microelectromechanical Systems*. Vol. 5, No. 1. Pg. 45. March 1996.

[4]Hecht, E. *Optics: Third Edition*. Addison Wesley Longman, Inc. Reading, Mass, 1998. Pg 420.

[5]Mao, H., J. Ke, P. Xing, Z. Lai. "Characterization of Micromechanical Optical Modulator" *Journal for Microelectromechanical Systems*. Vol. 10, No. 4 pg. 589. December 2001.

## ACKNOWLEDGEMENTS

The author acknowledges Dr. William Grande with advisement on processing and theory, Edward Furlani of Eastman Kodak Co. for theoretical simulation guidance, Dr. Bruce Smith with advisement on antireflective films, the RIT SMFL technicians (Scott Blondell, Bruce Tolleson, John Nash, Richard Battaglia, and Dave Yackoff) for technical support, Tom Grimsley for off-hours laboratory access, Charles Gruener for help in mask design, Kevin Munger, Chuck Faisst, Peter Gulvin of Xerox Corp. for processing advisement and Pete Terrana with SEM preparation.

**Matthew R. Shepard**, originally from Gloversville, NY, will receive his B.S in Microelectronic Engineering from Rochester Institute of Technology in 2003. He attained a co-op position at Motorola in Chemical Mechanical Planarization, and Photonics Corp. He is currently in search of a full-time position.